NMRF/RR/11/2024

RESEARCH REPORT

NWP Model Wind Speed Forecast Evolution for Optimized Wind Farm Operations

Priya Singh, Raghavendra Ashrit, Sushant Kumar

JULY 2024

National Centre for Medium Range Weather Forecasting

Ministry of Earth Sciences, Government of India

NWP Model Wind Speed Forecast Evolution for Optimized Wind Farm Operations

Priya Singh, RaghavendraAshrit, Sushant Kumar

National Centre for Medium Range Weather Forecasting

Ministry of Earth Sciences

A-50, Sector 62, NOIDA-201309, INDIA

July 2024

1	Name of the Institute	National Centre for Medium Range Weather Forecasting (NCMRWF)
2	Document Number	NMRF/RR/11/2024
3	Date of publication	July 2024
4	Title of the document	NWP Model Wind Speed Forecast Evolution for Optimized Wind Farm Operations
5	Type of Document	Research Report
6	No. of pages & Figures	28 Pages & 9 Figures
7	Number of References	23
8	Author (S)	Priya Singh, Raghavendra Ashrit, Sushant Kumar
9	Originating Unit	NCMRWF
10	Abstract	Wind Power Forecasting aids grid operators in balancing supply and demand, reduces the reliance on fossil fuel-based backup generation, and helps in the efficient management of energy storage systems. NWP models can provide forecasts ranging from hours to several days ahead, making them invaluable for both operational decision-making and strategic planning in the wind energy sector. The accuracy of Numerical Weather Prediction (NWP) data is one of the critical factors influencing wind power forecasts. This report evaluates the performance of NCMRWF Unified Model-Global (NCUM-G) and -Regional (NCUM-R) models for wind speed forecasts at three selected wind farms. The study has been performed considering the observed and predicted hourly winds for Jul-Dec 2023. Forecast accuracy is evaluated using standard statistical methods. The performance of the model in forecasting wind speed has been systematically evaluated on hourly, daily, and monthly temporal scales. The observed and forecasted wind data is found to be in good convergence, though the distribution of individual differences between observed and forecasted wind data indicated random error. Additionally, the study also assesses the effectiveness of bias correction, leading to

		improved wind speed forecasting, particularly at the Wind Farm2 (WF2) with higher forecast errors.
11	Security classification	Non-Secure
12	Distribution	Unrestricted Distribution
13	Key Words	Wind Power Forecast**,** Wind Farms, NWP Model, Surface winds, Wind Forecasts, Bias Correction

Table of Contents

NWP Model Wind Speed Forecast Evolution for Optimized Wind Farm Operations

Priya Singh, Raghavendra Ashrit, Sushant Kumar

सारांश

पवन ऊर्जा पूर्वानुमान ग्रिड ऑपरेटरों को आपूर्ति और मांग को संतुलित करने में सहायता करता है, जीवाश्म ईंधन-आधारित बैकअप उत्पादन पर निर्भरता कम करता है, और ऊर्जा भंडारण प्रणालियों के कुशल प्रबंधन में मदद करता है। एनडब्ल्यूपी मॉडल घंटों से लेकर कई दिनों तक का पूर्वानुमान प्रदान कर सकते हैं, जो उन्हें पवन ऊर्जा क्षेत्र में परिचालन निर्णय लेने और रणनीतिक योजना दोनों के लिए अमूल्य बनाता है। संख्यात्मक मौसम पूर्वानुमान (एनडब्ल्यूपी) डेटा की सटीकता पवन ऊर्जा पूर्वानुमानों को प्रभावित करने वाले महत्वपूर्ण कारकों में से एक है। यह रिपोर्ट तीन चयनित पवन फार्मों पर हवा की गति के पूर्वानुमान के लिए एनसीएमआरडब्ल्यूएफ यूनिफाइड मॉडल-ग्लोबल (एनसीयूएम-जी) और -रीजनल (एनसीयूएम-आर) मॉडल के प्रदर्शन का मूल्यांकन करती है। यह अध्ययन जुलाई-दिसंबर 2023 के लिए देखी गई और अनुमानित प्रति घंटा हवाओं को ध्यान में रखते हुए किया गया है। पूर्वानुमान सटीकता का मूल्यांकन मानक सांख्यिकीय तरीकों का उपयोग करके किया जाता है। हवा की गति का पूर्वानुमान लगाने में मॉडल के प्रदर्शन का प्रति घंटा, दैनिक और मासिक अस्थायी पैमानों पर व्यवस्थित रूप से मूल्यांकन किया गया है। प्रेक्षित और पूर्वानुमानित पवन डेटा अच्छे अभिसरण में पाया गया है लेकिन दोनों मॉडलों द्वारा कम आकलन की सामान्य प्रवृत्ति के साथ।इसके अतिरिक्त, अध्ययन पूर्वाग्रह सुधार की प्रभावशीलता का भी आकलन करता है, जिससे हवा की गति के पूर्वानुमान में सुधार होता है, विशेष रूप से उच्च पूर्वानुमान त्रुटियों के साथ पवनफार्म2 (WF2) पर।

कीवर्ड:पवनऊर्जा पूर्वानुमान, पवनफार्म, एनडब्ल्यूपीमॉडल, सतहीहवाएं, पवन पूर्वानुमान, पूर्वाग्रहसुधार

Abstract

Wind Power Forecasting aids grid operators in balancing supply and demand, reduces the reliance on fossil fuel-based backup generation, and helps in the efficient management of energy storage systems. NWP models can provide forecasts ranging from hours to several days ahead, making them invaluable for both operational decision-making and strategic planning in the wind energy sector. The accuracy of Numerical Weather Prediction (NWP) data is one of the critical factors influencing wind power forecasts. This report evaluates the performance of NCMRWF Unified Model-Global (NCUM-G) and -Regional (NCUM-R) models for wind speed forecasts at three selected wind farms. The study has been performed considering the observed and predicted hourly winds for Jul-Dec 2023. Forecast accuracy is evaluated using standard statistical methods. The performance of the model in forecasting wind speed has been systematically evaluated on hourly, daily, and monthly temporal scales. The observed and forecasted wind data is found to be in good convergence but with a general tendency of underestimation by both models. Additionally, the study also assesses the effectiveness of bias correction, leading to improved wind speed forecasting, particularly at the Wind Farm2 (WF2) with higher forecast errors.

Keywords: Wind Power Forecast, Wind Farms, NWP Model, Surface winds, Wind Forecasts, Bias Correction

1. Introduction:

Reliable wind power forecasting enables better scheduling of electricity generation, minimizes operational costs, and enhances the reliability of power systems. It aids grid operators in balancing supply and demand, reduces the reliance on fossil fuel-based backup generation, and helps in the efficient management of energy storage systems (Higashiyama et al., 2018). Inaccurate forecasts can lead to significant operational issues, including grid instability and increased costs due to the need for reserve power.

Wind power forecasting is essential for integrating wind energy into power grids, optimizing energy production, and ensuring grid stability. As the global demand for renewable energy sources escalates, accurate forecasting becomes increasingly critical. Wind energy, characterized by its variability and intermittency, poses unique challenges for both short-term and long-term prediction (Smith et al., 2007). NWP models have emerged as a pivotal tool in addressing these challenges, providing advanced methods for forecasting wind power.

NWP models use mathematical equations to simulate the atmosphere and predict weather conditions based on current and past observations. These models incorporate data from satellites, weather stations, and other sources to produce detailed forecasts of wind speed and direction, which are crucial for estimating wind power output. NWP models can provide forecasts ranging from hours to several days ahead, making them invaluable for both operational decision-making and strategic planning in the wind energy sector (Ernst et al., 2007). Recent advancements in NWP models have significantly improved their accuracy and reliability. Enhanced data assimilation techniques, higher spatial and temporal resolution, and the integration of ensemble forecasting have led to more precise predicti0ons of wind patterns (M. Leutbecher et al., 2008). These improvements are particularly beneficial in complex terrains and offshore environments where wind behaviour is more difficult to predict (Treiber et al., 2016).

The National Centre for Medium range Weather Forecast (NCMRWF) provides the NWP forecasts to the wind energy industry using a deterministic global model NCUM-G (Rajagopal et al. 2012, Kumar et al.2018, Rani et al., 2019) and a high-resolution regional model (Jayakumar

et al. 2019). The model forecast has been utilized in various sectorial application such as hydrology (Kumar et al., 2023), tropical cyclones (Kumar et al., 2022) and renewable energy (Rangaraj et al., 2024). The models have also been used in operational forecasting of tropical cyclones and an inter-comparison of model forecasts for Super Cyclone "Amphan" has been presented by (Ashrit et al., 2021). The near-surface wind speed, such as that at 10 and 50 m, and at 8 pressure levels, such as 1000, 995, 990, 985, 980, 975, 960, and 925 hPa, are calculated using the model outputs of U and V components of winds at these levels forecasted by NCMRWF models. Wind speed at these levels is then interpolated to turbine height for forecasting wind power.

In this study, we aim to provide a thorough evaluation of the NCMRWF global and regional model's performance in forecasting wind speed at three operational wind farms located in the southern state of Karnataka in India. Additionally, we propose a simple bias correction method that relies on real-time wind speed data from the wind farms. This approach is essential because uncertainties are inherent in the wind speed forecasts from NWP models, along with certain biases. The findings from this study will enhance the reliability and accuracy of NWP-based wind power forecasts over various time scales, thereby supporting the integration of more renewable energy into power grids while maintaining grid stability.

This report has been organized in the following ways: the NWP model details and datasets used in the study in section 2. Section 3 highlights the technical details of model evaluation, the statistical metrics used, and the bias correction method. In section 4 we have presented the model evaluation results and discussion of the study over selected wind farm locations. Finally, the results are summarized in section 5. We have also highlighted the limitations of our study at the end.

2. Description of NWP Model and Datasets

2.1 NWP Model Description

The NCUM-G model (George et al., 2016; Rajagopal et al., 2012) employs a seamless modeling approach, featuring a horizontal grid resolution of approximately 12 km and 70 vertical levels extending up to 80 km in altitude. Since 2018, it has been utilized for providing 240-hour

numerical weather forecasts (Kumar et al., 2018). The model and its assimilation system undergo periodic updates to incorporate advancements in scientific and technical fields. The model uses the advanced ENDGame dynamical core, which enhances the accuracy of solving primitive equations and reduces damping effects, leading to better variability in tropical regions and improved representation of tropical cyclones and other phenomena (Walters et al., 2017). For atmospheric analysis, NCUM employs the Hybrid 4D-Var data assimilation method, which integrates flow-dependent background errors provided by the Ensemble Transform Kalman Filter (ETKF) based on the NCUM ensemble prediction system (NEPS). The system places significant emphasis on assimilating Indian satellite data, including INSAT-3D Atmospheric Motion Vectors (AMV), Megha Tropiques (MT)-SAPHIR radiances, and Scatsat Ocean Surface Winds, along with other global observations. The NCUM global data assimilation system produces analyses four times daily at 0000, 0600, 1200, and 1800 UTC. Each 6-hour data assimilation cycle merges observations from a 6-hour window (centered ±3 hours around the analysis time) with the model background to generate the NCUM-G analysis. For detailed information on model parameterization schemes and data assimilation processes, refer to Kumar et al., (2018).

The NCUM-R model features a horizontal grid resolution of approximately 4 km and 80 vertical levels, with the model top at 38.5 km and 14 levels below 1 km. It operates at a 1-minute run time step. Covering India and adjacent oceanic areas, the model provides 72-hour forecasts. This convection-permitting configuration does not parameterize sub-grid scale deep convection. It uses the prognostic cloud fraction and condensate (PC2) scheme based on (Wilson et al., 2008). The sub-grid turbulence is modeled using a blended scheme (Boutle et al., 2014), which dynamically combines the 1D boundary-layer scheme by (Lock et al., 2000) with a 3D Smagorinsky scheme, utilizing a mixing factor of 0.5. For orography, the model employs the 90 m digital elevation map from the NASA Shuttle Radar Topographic Mission (SRTM). High-resolution analysis is generated by the 4D-Var data assimilation system, which includes observations used in the NCUM global system (though with different data thinning strategies). Additionally, Indian Doppler Weather Radar radial wind data is incorporated into the regional data assimilation system within a ± 3 h time window. The model domain spans the South Asian region, including the Bay of Bengal and parts of the Arabian Sea (6°S to 41°N and 62°E to 106°E). Further details on the NCUM-R model configuration are available in (Bush et al., 2020; Dutta et al., 2019; Jayakumar et al., 2020).

2.2 Data Description

Model Data: NCUM-G and NCUM-R produce forecasts of u and v components of near-surface wind speed at 50-m level, 1-hr time intervals from the recent time period July 2023 to December 2023. Model forecasts generated at 00 UTC run up to 120 h forecast length have been evaluated against observed data. The focus of the study revolves around three wind farms (WF) sites, WF1, WF2, and WF2, represented in Figure 1. The details of the WF in terms of latitude, longitude, and average elevation are presented in Table 1(a) for the NCUM-G model and Table 1(b) for the NCUM-R model.

Site Observation: Site observations have been provided by an Independent Power Producing (IPP) company for three wind farms located in the Karnataka state of India. The location of wind turbine generators (WTG) for these wind farms has been presented in Figure 1. There are 31, 15, and 40 WTGs installed over the WF1, WF2, and WF3, which have an average elevation of 872m, 954m, and 939 m, respectively. These WTGs are manufactured by Enercon, having a capacity of 0.8 MW, a hub height of 56m, a rotor diameter of 48 m, and a model mix of E48 (70 numbers) and E50 (16 numbers). The anemometer installed over these WTGs provides the wind speed and is transmitted through SCADA at 15-minute intervals. For the model evaluation purpose, the instantaneous hourly wind speed of all WTGs for each wind farm has been averaged. The time steps have been considered in such a way that it matches the time-step of the model forecasts, i.e., 1:30, 2:30, 3:30….23:30 h.

3. Methodology

3.1 Statistical measures for inter-comparison of observed and predicted

Statistical metrics such as BIAS, MAE (mean absolute error), RMSE (root mean square error), CC (correlation coefficient) have been computed using the equations/formulae as follows:

$$\text{MAE}=\frac{1}{n}\sum_{i=1}^{n}|Observed_i - Forecast_i| \quad (1)$$

$$\text{RMSE}=\sqrt{\frac{1}{n}\sum_{i=1}^{n}(Observed_i - Forecast_i)^2} \quad (2)$$

$$CC=\frac{\sum_{i=1}^{n}\left(Observed_i-\overline{Observed}\right)\left(Forecast_i-\overline{Forecast}\right)}{\sqrt{\sum_{i=1}^{n}\left(Observed_i-\overline{Observed}\right)^2\sum_{i=1}^{n}\left(Forecast_i-\overline{Forecast}\right)^2}} \quad (3)$$

$$MBE = 1/n\sum_{i=1}^{i=n}(Forecast - observed) \quad (4)$$

Where, n is the length of the datasets being compared, Forecast and Observed values correspond to NCMRWF Seasonal Prediction System (NSPS) model forecast and analysis respectively, whereas Forecast and Observed represent the mean values of it.

3.2 Bias correction

NWP model forecasts face inherent challenges stemming from imperfect initial conditions, numerical approximations, and the simplification of numerous atmospheric processes, all contributing to specific biases (Cheng and Steenburgh, 2005; Coleman et al., 2010; Kalman R.E., 1960) which are more prominent for surface and boundary-layer parameters such as winds (Cheng et al., 2013). This study aims to rectify the bias in the forecasts of wind speed from the NWP model for the period July 2023 to December 2023. This correction process involves the application of a technique outlined below:

We implemented a linear regression-based bias correction (Do-Yong Kim et al., 2012) methodology to refine forecasted data over a continuous six-month observational period. The hourly observed data O(t) and corresponding forecasted data F(t) were utilized, where t represents the time index. Our approach involved training the bias correction model using a rolling window technique: initially, a three-day (72 hours) subset of data was used to estimate the linear relationship between observed and forecasted values. This relationship is expressed as:

$$O(t)=\alpha F(t)+\beta O(t) \quad (5)$$

where α and β are the slope and intercept parameters of the linear regression model, respectively.

Following model calibration, the estimated coefficients α and β were then applied to correct the forecast bias for the subsequent 24-hour period:

$$\text{Corrected Forecast}(t)=(O(t)-\beta)/\alpha \quad (6)$$

This moving bias correction procedure was iteratively performed throughout the entire study period to continuously update the regression coefficients using newly available data. By employing this iterative approach, we aimed to systematically minimize discrepancies between observed and forecasted values, thereby enhancing the accuracy and reliability of the forecasted data for the study's scientific analysis and conclusions.

4. Results and discussions

4.1 NWP Model Evaluation

The focus of the study revolves around three selected Indian Wind Farms (WF) sites represented in Figure1with corresponding model orography also illustrated in the same figure. From the figure, we can infer that the WF are at relatively higher elevation in NCUM-G model as compared to NCUM-R. Specifically, WF1 and WF3 are at relatively lower elevation whereas WF2 is located at the highest elevation. The local topography affects the weather phenomenon which at many instances may not be well represented by the NWP models due to their coarser resolution.

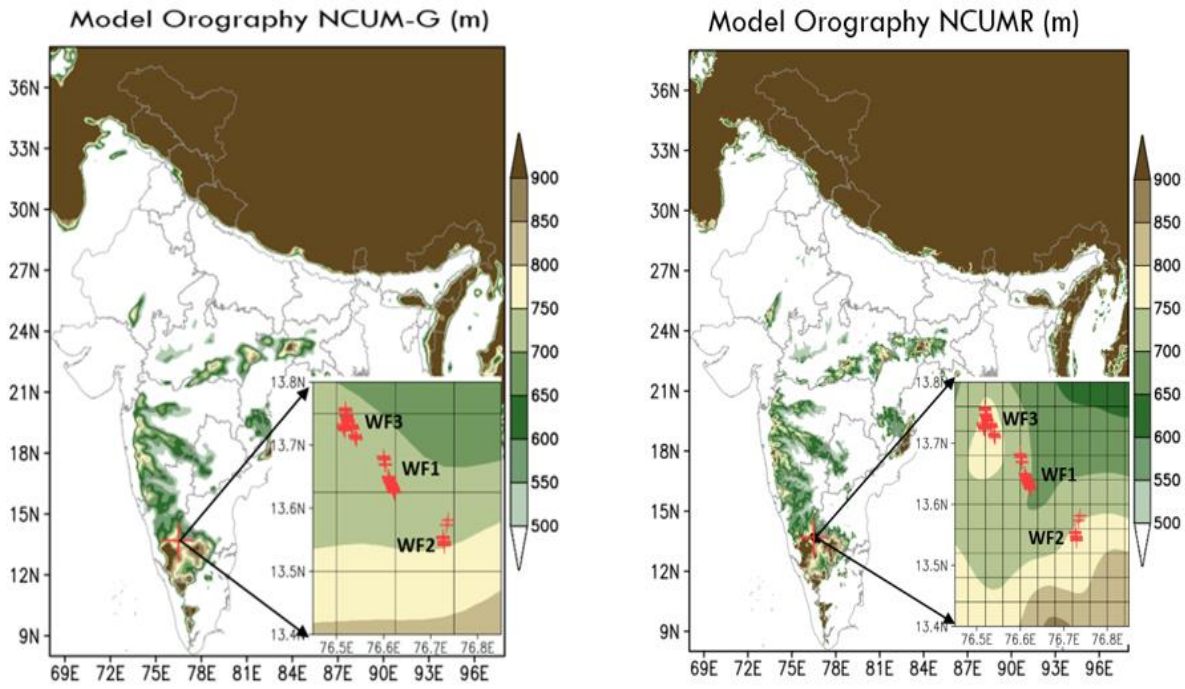

Figure1: Model orography that highlights the terrain at selected WF sites.

The details of the WF in terms of latitude, longitude, and the average elevation are presented in Table 1(a) for NCUM-G model and Table 1(b) for NCUM-R model.

Table 1(a)NCUM-G model points

Wind Farm	Latitude	Longitude	Elevation(m)
WF1	76.62	13.62	726
WF2	76.75	13.50	750
WF3	76.50	13.75	701

Table 1(b)NCUM-R model points

Wind Farm	Model –Grid Latitude	Model –Grid Longitude	Elevation(m)
WF1	76.6	13.64	713
WF1	76.6	13.68	726
WF2	76.72	13.56	757
WF3	76.52	13.72	756
WF3	76.52	13.76	751

The NWP model outputs U and V components of winds at 50 m above ground level, which were utilized to compute wind speed (WS). Figure 2 illustrates the mean WS observed during the study period, facilitating a comparative analysis between forecasted and analysed parameters. The spatial distribution of forecasted wind speeds generally aligns well with the observed patterns. Across the study area, mean wind speeds consistently exceed 4-6 m/s in most of the western parts of India and remain below 4 m/s in the eastern regions. Whereas specific regions within Rajasthan and Gujarat exhibit even more elevated wind speeds, exceeding 8 m/s. The NWP model generally performs well in forecasting wind speeds across India, careful consideration is necessary when interpreting results for specific regions, particularly those with complex topography. However, notable discrepancies are evident, primarily in Rajasthan, Gujarat and Karnataka, where the model tends to overestimate wind speeds. This overestimation is particularly pronounced in specific localized areas. These findings underscore the model's

overall competence in capturing the broad spatial patterns of wind speed across the region while highlighting the need for improved accuracy, especially in localized forecasting over complex terrains.

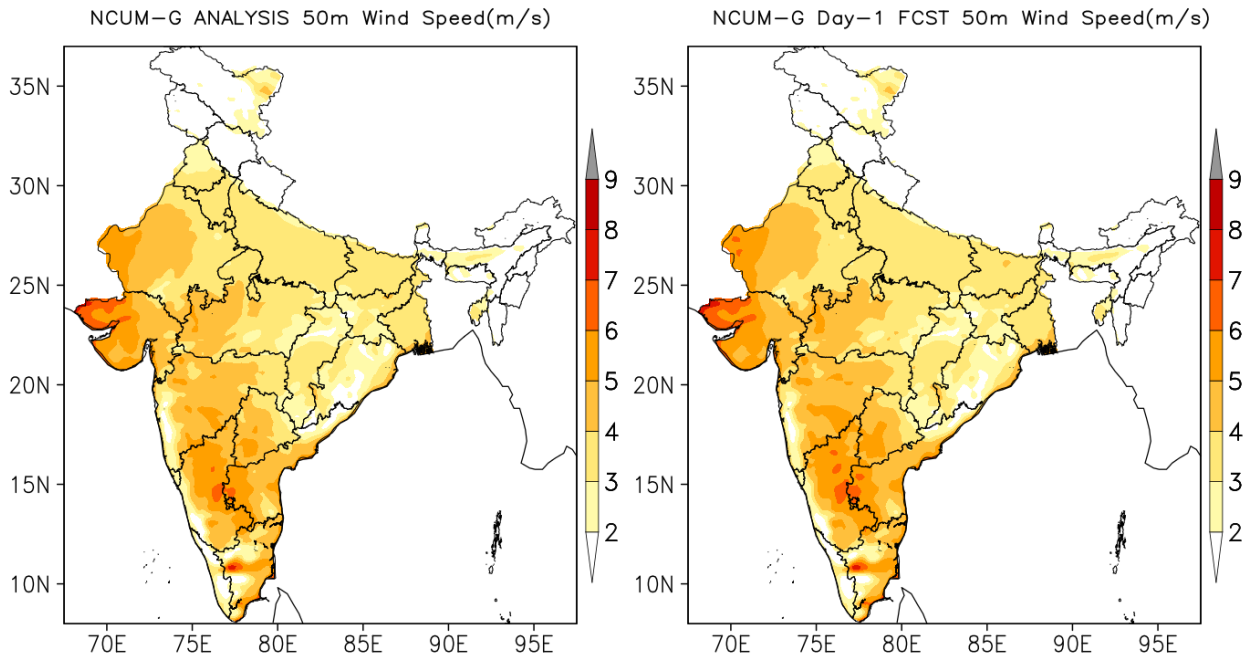

Figure 2: Wind Speed Plot comparing NCUM-G model Day 1forecast to analysis wind speed for the period July 2023 to December 2023.

Figure 3 provides a comprehensive assessment of the MBE, MAE, and RMSE for wind speed (WS) forecasts compared to model analysis spanning from July 2023 to December 2023. For the Day 1 forecast period, the RMSE across most of India remains below 1.2 m/s, indicating generally accurate predictions. The MAE is below 0.8 m/s, reflecting minor absolute errors, and the MBE ranges between -0.8 to 0.8 m/s. However, certain regions in Rajasthan, Gujarat, Punjab, Haryana, and Uttar Pradesh exhibit slightly higher RMSE values, ranging up to 1.5 m/s. The MAE in these areas ranges up to 1 m/s, indicating somewhat larger absolute errors, and the MBE ranges between 0.4 to 0.6 m/s, suggesting a moderate bias towards overestimation. These findings highlight a notable discrepancy between forecasted and analysis wind speeds in these specific regions. Despite this, the overall accuracy of the model forecasts for the first 24 hours (Day 1) is reasonably good across the study period. While the NWP model demonstrates

promising accuracy in forecasting wind speeds over broad spatial scales, targeted improvements are necessary to refine predictions in regions prone to higher error rates.

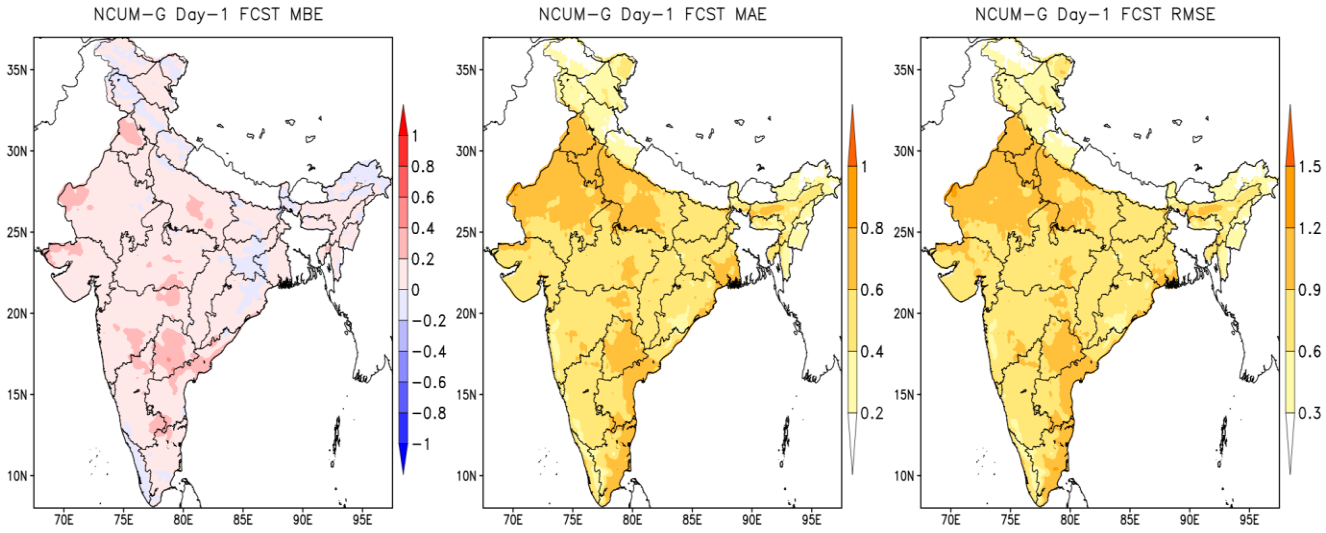

Figure 3. MBE, MAE, and RMSE in Day 1 forecasts in comparison to model analysis, spanning the period July 2023 to December 2023.

Figure 4 provides a detailed examination of the seasonal dependency in wind speed (WS), presenting the monthly cycle of observed and forecasted WS data from July 2022 to December 2023 for three wind farms (WF). The comparison reveals a notably strong agreement between forecasted and observed WS across the three WF sites, with WF1 and WF3 showing particularly close matches for WF1 and WF3 as compared to WF2. This variation in performance can be attributed to factors such as geographical location and local topography, which influence the accuracy of wind speed predictions at specific sites. The figure offers a comprehensive overview of mean WS across seasons, facilitating clear comparisons between the different WFs and highlighting significant seasonal patterns. Notably, the highest mean WS are observed during the months of July to September, characterized as the high wind season, while the lowest mean WS occur from September to December, identified as the low wind season. The results indicate that the Day 1 forecast closely aligns with observed data, demonstrating a high level of accuracy in short-term WS predictions. However, biases in the forecasts are particularly prominent during the high wind season from July to September, suggesting potential areas for model improvement

or calibration. Overall, these findings underscore the seasonal variability in WS and the robustness of the NWP model in capturing these variations across different geographical and climatic conditions. They also emphasize the importance of site-specific considerations in interpreting forecast accuracy, particularly in regions prone to seasonal fluctuations in wind patterns.

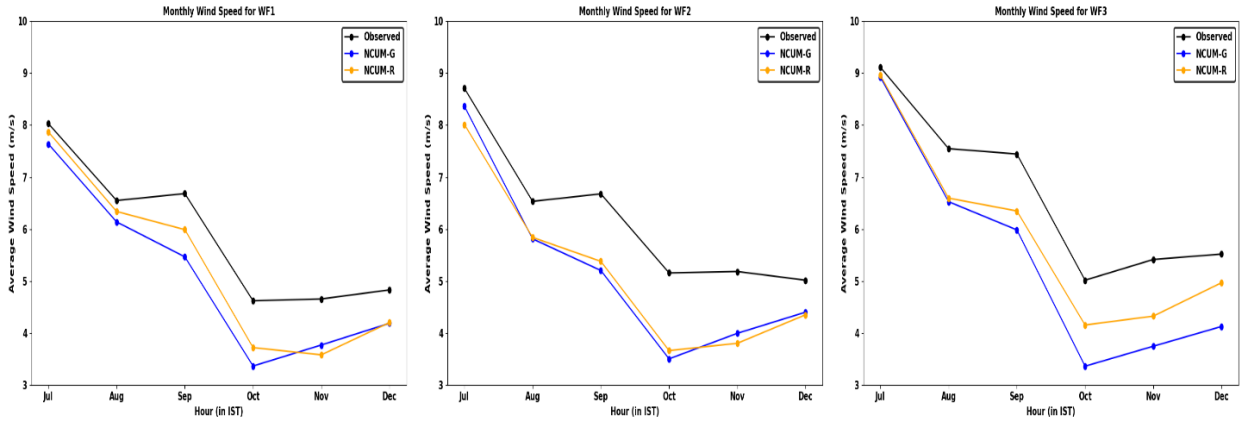

Figure4: Monthly cycle of the observed and forecast wind speed averaged over each of the three WF sites during July 2023 to December 2023.

A comprehensive analysis has been conducted of daily time series data for observed and forecasted wind speeds across three WF sites for the period of July 2023 to December 2023. It provides valuable insights into the temporal dynamics of wind speeds across different seasons and their implications for wind energy management. The analysis of daily time series data underscores the importance of robust forecasting models capable of handling rapid changes in wind speed. During the study period, WS exhibit significant variability across seasons (Figure 4). The months of July to September were identified as the high wind season (HWS) (above panel of Figure 5), characterized by the highest mean wind speeds observed at all WF sites. Conversely, from October to December, WS were lowest, marking the low wind season (LWS) (bottom panel of Figure 5). This seasonal pattern is consistent with typical meteorological conditions in the region, reflecting broader atmospheric circulation patterns influencing wind patterns. Our analysis of daily time series data highlighted pronounced fluctuations in wind speeds within both HWS and LWS. These fluctuations were observed consistently across all WF sites and were effectively captured by both NCUM-G and NCUM-R models. Notably, both models

demonstrated the ability to capture sudden increases and decreases in wind speeds within a single day, indicating their capability to handle rapid changes in atmospheric conditions. The observed abrupt changes in daily wind speeds underscore the complexity and challenges associated with wind speed forecasting. The ability of forecast models to accurately predict these rapid fluctuations is crucial for optimizing the operational efficiency of wind farms and integrating wind energy into the power grid effectively.

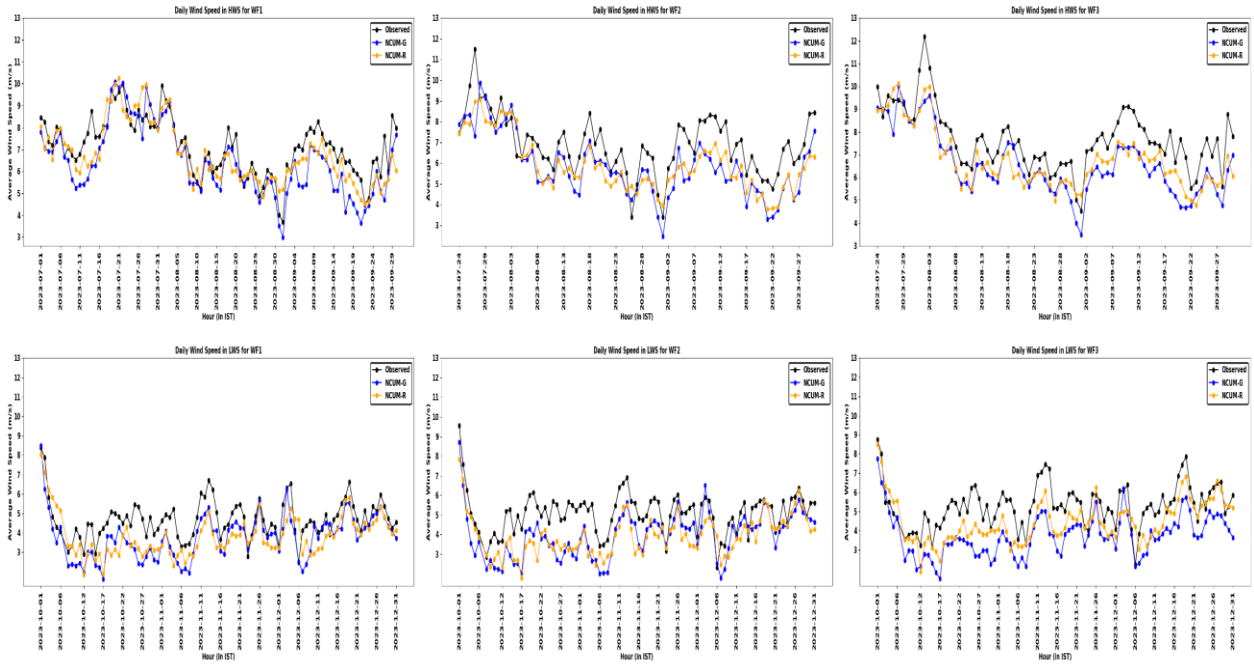

Figure5: Daily time series of the observed and forecast wind speed for each of the three WF sites during July 2023 to December 2023.

The mean diurnal variation of hourly wind speeds across the WF sites have been presented in Figure 6. The data reveals a compelling pattern in the fluctuations of wind speed throughout a typical day. The findings indicate that the wind speeds exhibit a consistent rhythm with lower values during the early morning and a gradual increase through the day, peaking in the late afternoon. The findings indicate that both the model forecasts are generally effective in capturing these diurnal patterns throughout the day. However, it is noted that there is a higher range of bias observed during the early morning and late night periods. The model tends to underestimate wind speeds during these times, potentially due to factors such as boundary layer dynamics or local meteorological effects not fully accounted for in the modelling process. Nevertheless, the

models demonstrate accurate forecasts during periods when wind speeds peak, which are crucial for operational planning in wind energy generation. This highlights the models capability to predict wind conditions accurately during times of maximum potential energy production. The observed diurnal variations underscore the importance of temporal accuracy in wind speed forecasting, particularly for optimizing energy capture and operational scheduling at WF sites. Future improvements in modelling techniques could focus on refining predictions during periods of lower wind speeds, thereby enhancing the overall reliability and utility of wind energy forecasting systems.

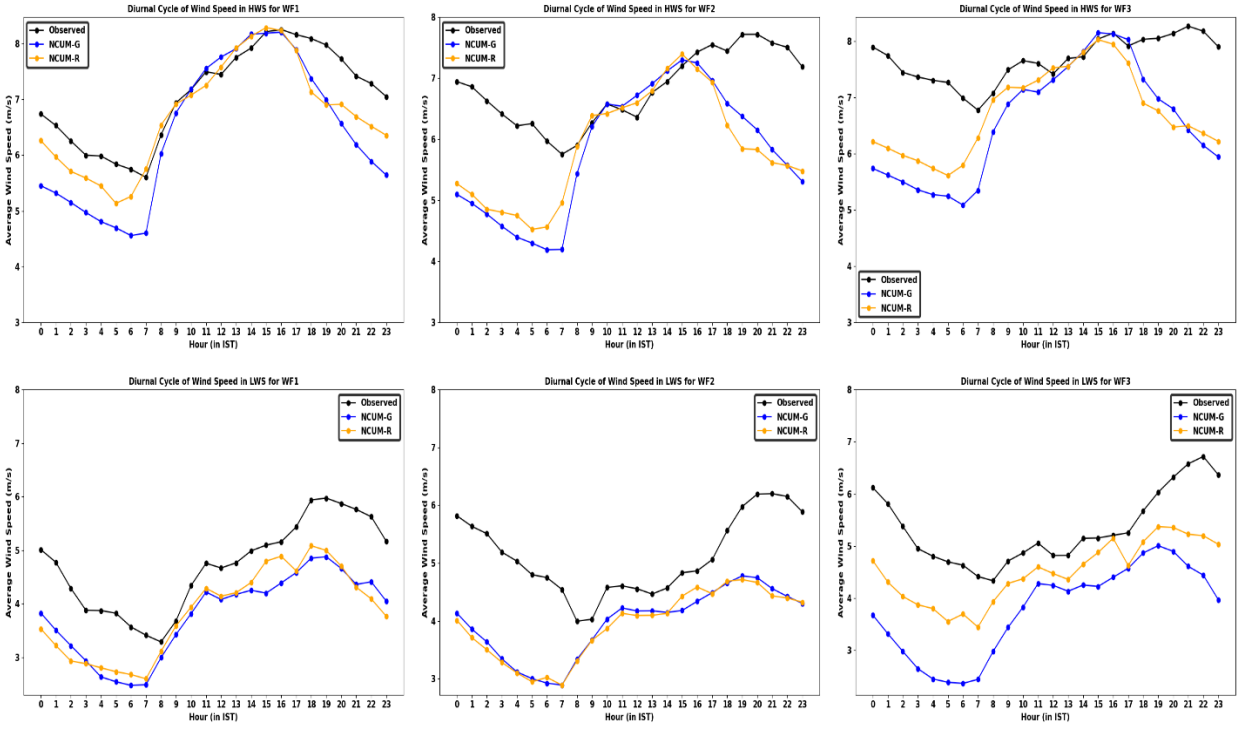

Figure 6: Mean diurnal cycle of the analysed and forecast wind speed averaged over each of the three WF sites during July 2023 to December 2023.

The diurnal variation of Mean Absolute Error (MAE) in hourly wind speeds was examined across three WF sites, as depicted in Figure 7. A distinct pattern in wind speed fluctuations over a typical day emerged, revealing a consistent rhythm characterized by higher MAE values during early morning and late night periods when wind speeds were generally low (see Figure 6). Conversely, MAE values were lower in the late afternoon, corresponding to periods of higher

wind speeds (see Figure 6). Specifically, at WF3 in LWS, significant errors exceeding 1.8 m/s were observed during the early morning and late night periods for forecasts generated by the NCUM-G model. These findings underscore the challenges in accurately predicting wind speeds during periods of minimal wind activity, highlighting potential areas for model refinement or additional data assimilation strategies. These insights into the temporal dynamics of wind speed variability across WF sites are crucial for optimizing wind energy generation and improving the reliability of forecasting models.

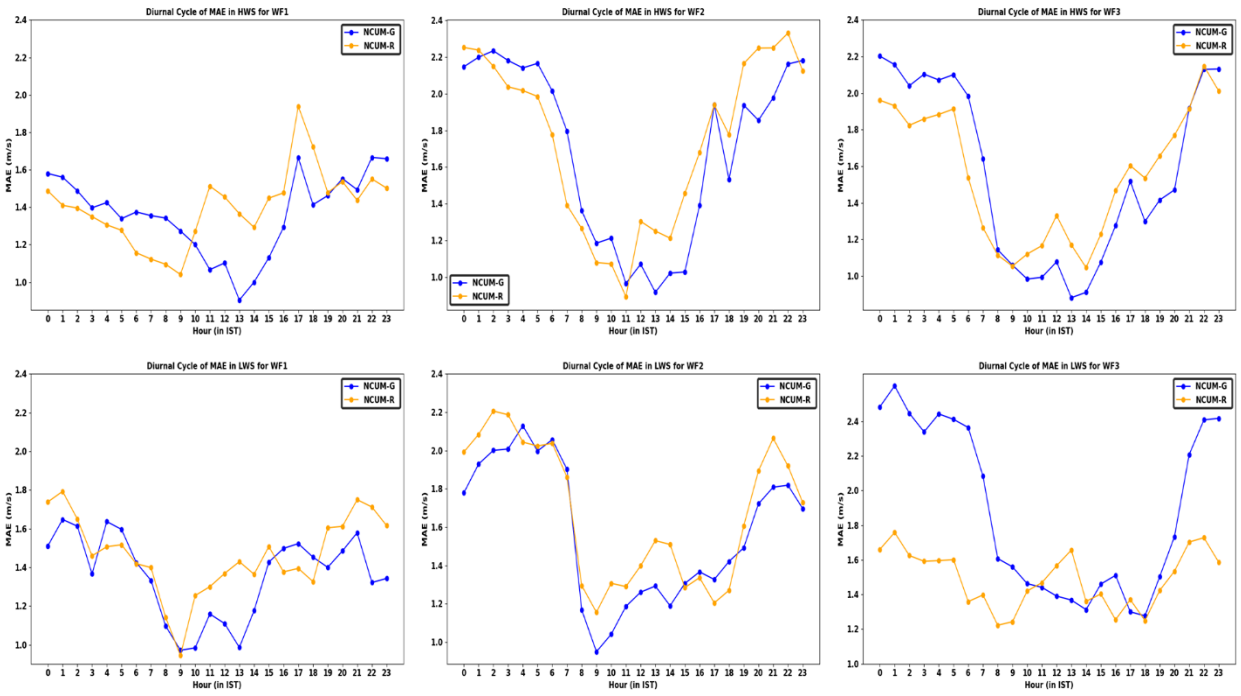

Figure 7: Diurnal variation in the MAE in forecast and observed wind speed for each of three WF sites, spanning the period from July2023 to December 2023.

Figure 8 presents scatter plots illustrating the relationship between observed and forecasted (Day-1) wind speeds across three WF sites from July 2022 to December 2023. The upper panels depict data from the HWS spanning July to September, while the lower panels show data from the LWS from October to December. Results are shown for two NWP models: NCUM-G and NCUM-R. Across all WF sites and seasons, the scatter plots demonstrate a notably strong association between observed and forecasted wind speeds. Each plot exhibits a high level of correlation, as indicated by the high R^2 values. Comparatively, the NCUM-G model generally

shows a stronger association between observed and forecasted wind speeds than the NCUM-R model. This difference underscores the varying performance of different NWP models in capturing wind speed dynamics. Furthermore, the association between observed and forecasted wind speeds is consistently higher during the high wind season compared to the low wind season. This suggests that the forecasting model performs particularly well when predicting wind speeds during periods of higher atmospheric variability and stronger winds. These findings underscore the effectiveness and reliability of the forecasting approach employed in accurately predicting wind speeds at each WF site. Such accuracy is crucial for informed decision-making and operational planning in the context of wind power generation. In conclusion, the robust correlation between observed and forecasted wind speeds reaffirms the model's accuracy and reliability, highlighting its potential utility in various practical applications, including energy production forecasting and environmental monitoring.

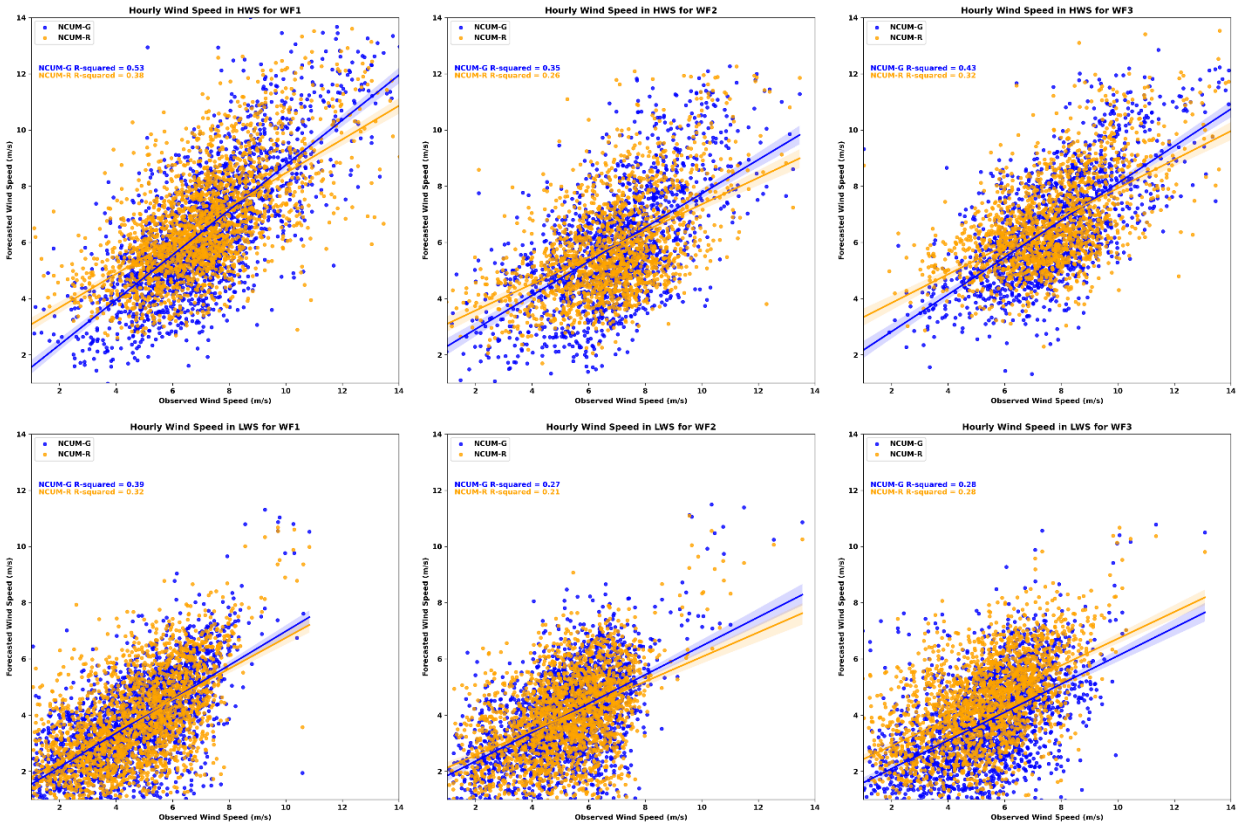

Figure 8: Scatter plot of observed Vs forecast hourly wind speed (m/s) for each of the three WF sites during July 2023 to December 2023. The plots indicate very good association as indicated by R^2 values in each panel.

The frequency distribution of wind speed (WS) across various categories to assess the accuracy of Day-1 forecasts and to identify potential biases or discrepancies. Figure 9 presents these distributions, divided into high wind speed (HWS) in the upper panel and low wind speed (LWS) in the lower panel. Both NWP models successfully captured the overall distribution patterns, albeit with some degree of underestimation. Specifically, during the HWS, the observed data exhibited a peak in wind speeds ranging from 7 to 9 m/s, whereas both models consistently forecasted a peak in the 5 to 7 m/s range. Similarly, in the LWS, observed data indicated a peak between 4 to 6 m/s, whereas the forecasts showed a peak between 3 to 5 m/s. Notably, compared to NCUM-R, the NCUM-G model demonstrated closer alignment with the observed WS distributions. These findings suggest that while the models generally captured the broad trends in WS distribution, there was a tendency towards underestimating peak wind speeds in both HWS and LWS conditions.

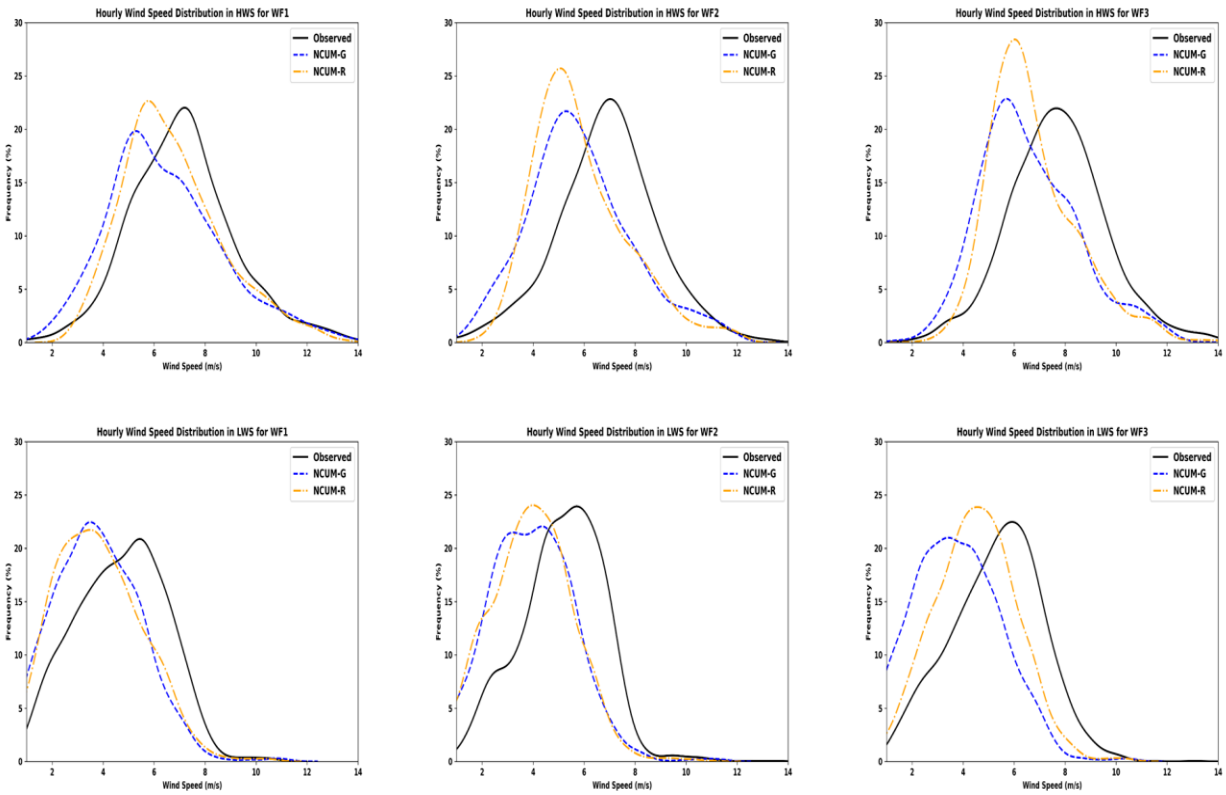

Figure 9: Frequency distribution (%) of observed and Forecast (Day-1) wind speed for each WF sites, spanning the period from July2023 to December 2023.

4.2 Bias Correction

The analysis conducted in the model verification section strongly underscores the essential need for bias correction in forecasting. In this section we have attempted to reduce the model biases in forecast wind speed adopting the linear regression bias correction techniques following the methodology described in section 3. The skill assessment has been done in terms of MAE and RMSE in the wind speed. In Table 2(a) the MAE and in Table 2(b) the RMSE in the day 1 forecast from the models (NCUM-G and NCUM-R) before and after bias-correction have been presented. The variability of the error clearly shows that where the errors in model forecasts are relatively higher are appreciably reduced. The bias correction also helps achieve lower errors over the WF2 in particular where the mean error was comparatively high from other two wind farms. This concludes that a simple bias correction technique is helpful and efficient aligning the wind speed forecast to the observed WS.

In the model verification section 4.1, our study emphasizes the critical necessity for bias correction in wind speed forecasting. We employed linear regression bias correction techniques as outlined in Section 3 to mitigate model biases in wind speed forecasts. The effectiveness of this approach was evaluated through skill assessment metrics, specifically Mean Absolute Error (MAE) and Root Mean Square Error (RMSE), which were computed for the day 1 forecasts from two models, NCUM-G and NCUM-R, both before and after bias correction. Table 2(a) presents the MAE values, while Table 2(b) displays the RMSE values. These tables highlight how the variability of errors in model forecasts was notably reduced post-correction, particularly in instances where initial errors were comparatively higher. Notably, the application of bias correction resulted in lower errors, particularly evident for WF2, where the mean error was initially pronounced compared to the other two wind farms. The findings underscore the efficacy of simple bias correction techniques in aligning wind speed forecasts more closely with observed values. This alignment is crucial for enhancing the reliability and accuracy of wind energy forecasts, thereby supporting better-informed decision-making in energy resource management and operational planning. Future research could further explore advanced bias correction

methodologies and their integration into operational forecasting systems to continually refine and optimize wind speed predictions.

Table2(a): Comparison of MAE in Day 1 forecasts before and after bias correction, relative to observed data, for HWS(July 2023 to September 2023).

	Before BC MAE		After BC MAE		Before BC RMSE		After BC RMSE	
	NCUM-G	NCUM-R	NCUM-G	NCUM-R	NCUM-G	NCUM-R	NCUM-G	NCUM-R
WF1	1.36	1.39	1.10	1.25	1.75	1.77	1.43	1.60
WF2	1.71	1.74	1.32	1.36	2.13	2.13	1.70	1.77
WF3	1.60	1.58	1.19	1.29	1.98	1.96	1.52	1.65

Table2(b): Comparison of MAE in Day 1 forecasts before and after bias correction, relative to observed data, for LWS(September 2023 to December 2023).

	Before BC MAE		After BC MAE		Before BC RMSE		After BC RMSE	
	NCUM-G	NCUM-R	NCUM-G	NCUM-R	NCUM-G	NCUM-R	NCUM-G	NCUM-R
WF1	1.36	1.48	1.14	1.22	1.76	1.86	1.44	1.54
WF2	1.57	1.68	1.15	1.20	1.98	2.10	1.47	1.53
WF3	1.88	1.49	1.24	1.27	2.31	1.86	1.56	1.59

5. Conclusions

5.1 The model's overall competence in capturing the broad spatial patterns of wind speed across India while highlighting the need for improved accuracy, especially in localized forecasting over complex terrains.

5.2 The model forecast accuracy in the first 24 hours (Day1) is reasonably good, with a RMSE of less than 1.5 m/s and MAE of less than .8 m/s for Pan-India predictions.

5.3 The wind speed data reveals notable seasonal patterns, with the highest mean wind speeds are observed during the months July to September, which can be characterized as the high wind season and lowest mean wind speeds are observed during the months September to December,

which can be characterized as the low wind season. Further, the study reveals that biases are particularly prominent during the HWS.

5.4 The mean diurnal variation of hourly wind speed exhibits a consistent pattern with lower values during the early morning and a gradual increase through the day, peaking in the late

5.5 The scatter plots depict a high level of association between analysis and forecasted (Day 1) wind speed, as seen by the high values of R^2. This robust correlation confirms the accuracy and reliability of the utilized forecasting model.

5.6 The Day-1 forecast distribution for each wind speed range closely matched the observed WS, indicating reliability in the forecasting approach.

5.7 The diurnal variation in MAE in Day-1 wind speed forecasts compared to observed WS revealed consistently low MAE values across all WF sites, with each site exhibiting MAE values below 2 m/s.

5.8 Linear regression bias correction technique significantly reduces errors in model forecasts, particularly evident for WF2, where the mean error was initially pronounced compared to the other two wind farms.

Limitations

The report thoroughly examines the performance of NCMRWF Unified Model-Global (NCUM-G) and -Regional (NCUM-R) models in forecasting wind speed, highlighting the importance of implementing bias correction for accurate forecasts. We have introduced a straightforward approach and achieved satisfactory results in bias correcting wind speed. Additionally, we plan to explore a more advanced technique utilizing machine learning algorithms. Another approach we intend to explore involves bias correction of both the u and v components of winds, leading to improved forecasts of wind speed crucial forwind power forecasts.

Authors Contribution: Data Curation and Analysis, Methodology, and manuscript writing by Priya Singh.The report was conceptualized, reviewed and supervised by Dr. Raghavendra Ashrit. Sushant Kumar contributed to conceptualization and manuscript writing.

References:

1. Ashrit, R., Kumar, S., Dube, A., Arulalan, T., Karunasagar, S., Routray, A., Mohandas, S., George, John.P., Mitra, A.K., 2021. Tropical cyclone forecast using NCMRWF Global (12 km) and regional (4 km) models. MAUSAM 72, 129–146. https://doi.org/10.54302/mausam.v72i1.125
2. Boutle, I.A., Eyre, J.E.J., Lock, A.P., 2014. Seamless Stratocumulus Simulation across the Turbulent Gray Zone. Mon. Weather Rev. 142, 1655–1668. https://doi.org/10.1175/MWR-D-13-00229.1
3. Bush, M., Allen, T., Bain, C., Boutle, I., Edwards, J., Finnenkoetter, A., Franklin, C., Hanley, K., Lean, H., Lock, A., Manners, J., Mittermaier, M., Morcrette, C., North, R., Petch, J., Short, C., Vosper, S., Walters, D., Webster, S., Weeks, M., Wilkinson, J., Wood, N., Zerroukat, M., 2020. The first Met Office Unified Model–JULES Regional Atmosphere and Land configuration, RAL1. Geosci. Model Dev. 13, 1999–2029. https://doi.org/10.5194/gmd-13-1999-2020
4. Cui, B., Toth, Z., Zhu, Y., Hou, D., 2012. Bias Correction for Global Ensemble Forecast. Weather Forecast. 27, 396–410. https://doi.org/10.1175/WAF-D-11-00011.1
5. Dutta, D., Routray, A., Preveen Kumar, D., George, J.P., Singh, V., 2019. Simulation of a heavy rainfall event during southwest monsoon using high-resolution NCUM-modeling system: a case study. Meteorol. Atmospheric Phys. 131, 1035–1054. https://doi.org/10.1007/s00703-018-0619-0
6. Ernst, B., Oakleaf, B., Ahlstrom, M., Lange, M., Moehrlen, C., Lange, B., Focken, U., Rohrig, K., 2007. Predicting the Wind. IEEE Power Energy Mag. 5, 78–89. https://doi.org/10.1109/MPE.2007.906306
7. George, J.P., S. Indira Rani, A. Jayakumar, Saji Mohandas, Mallick, S., R. Rakhi, M. N. R. Sreevathsa, E. N. Rajagopal, 2016. NCUM Data Assimilation System. https://doi.org/10.13140/RG.2.1.3576.2167
8. Higashiyama, K., Fujimoto, Y., Hayashi, Y., 2018. Feature Extraction of NWP Data for Wind Power Forecasting Using 3D-Convolutional Neural Networks. Energy Procedia 155, 350–358. https://doi.org/10.1016/j.egypro.2018.11.043

9. Jayakumar, A., Abel, S.J., Turner, A.G., Mohandas, S., Sethunadh, J., O'Sullivan, D., Mitra, A.K., Rajagopal, E.N., 2020. Performance of the NCMRWF convection-permitting model during contrasting monsoon phases of the 2016 INCOMPASS field campaign. Q. J. R. Meteorol. Soc. 146, 2928–2948. https://doi.org/10.1002/qj.3689
10. Kumar, K.N., Ashrit, R., Kumar, S., Johney, C., J., 2023. Evaluation of Quantitative Precipitation Forecast Performance of NWP models in Indian River Basins (Scientific No. NMRF/RR/03/2023). NOIDA.
11. Kumar, S., Jayakumar, A., Bushair, M.T., Buddhi, P., george, gibies, Lodh, A., Rani, S.I., George, J.P., 2018. Implementation of New High Resolution NCUM Analysis-Forecast System in Mihir HPCS (Technical No. NMRF/TR/01/2018). NCMRWF.
12. Kumar, Sushant, Dube, A., Kumar, Sumit, Rani, S.I., Sharma, K., Karunasagar, S., Mohandas, S., Ashrit, R., George, J.P., Mitra, A.K., 2022. Improved skill of NCMRWF Unified Model (NCUM-G) in forecasting tropical cyclones over NIO during 2015–2019. J. Earth Syst. Sci. 131, 114. https://doi.org/10.1007/s12040-022-01869-2
13. Lock, A.P., Brown, A.R., Bush, M.R., Martin, G.M., Smith, R.N.B., 2000. A New Boundary Layer Mixing Scheme. Part I: Scheme Description and Single-Column Model Tests. Mon. Weather Rev. 128, 3187–3199. https://doi.org/10.1175/1520-0493(2000)128<3187:ANBLMS>2.0.CO;2
14. Leutbecher M., Palmer T.N.,2008. Ensemble forecasting. Journal of Computational Physics 227 (2008) 3515–3539.
15. Rajagopal, E.N., Iyengar, G.R., George, J.P., dasgupta, munmun, Mohandas, S., Siddharth, R., Gupta, A., Sharma, K., prasad, v. s., 2012. Implementation of the UM model based analysis-forecast system at NCMRWF (Technical), NMRF/TR/2/2012. NCMRWF.
16. Rangaraj, A., Srinath, Y., Boopathi, K., D M, R.P., Kumar, S., 2024. Statistical post-processing of numerical weather prediction data using distribution-based scaling for wind energy. Wind Eng. 0309524X241238353. https://doi.org/10.1177/0309524X241238353
17. Rani, S.I., Taylor, R., Sharma, P., Bushair, M.T., Jangid, B.P., George, J.P., Rajagopal, E.N., 2019. Assimilation of INSAT-3D imager water vapour clear sky brightness

temperature in the NCMRWF's assimilation and forecast system. J. Earth Syst. Sci. 128, 197. https://doi.org/10.1007/s12040-019-1230-6

18. Singh, H., Dube, A., Kumar, S., Ashrit, R., 2020. Bias correction of maximum temperature forecasts over India during March–May 2017. J. Earth Syst. Sci. 129, 13. https://doi.org/10.1007/s12040-019-1291-6
19. Smith, J.C., Milligan, M.R., DeMeo, E.A., Parsons, B., 2007. Utility Wind Integration and Operating Impact State of the Art. IEEE Trans. Power Syst. 22, 900–908. https://doi.org/10.1109/TPWRS.2007.901598
20. Treiber, N.A., Heinermann, J., Kramer, O., 2016. Wind Power Prediction with Machine Learning, in: Lässig, J., Kersting, K., Morik, K. (Eds.), Computational Sustainability, Studies in Computational Intelligence. Springer International Publishing, Cham, pp. 13–29. https://doi.org/10.1007/978-3-319-31858-5_2
21. Walters, D., Boutle, I., Brooks, M., Melvin, T., Stratton, R., Vosper, S., Wells, H., Williams, K., Wood, N., Allen, T., Bushell, A., Copsey, D., Earnshaw, P., Edwards, J., Gross, M., Hardiman, S., Harris, C., Heming, J., Klingaman, N., Levine, R., Manners, J., Martin, G., Milton, S., Mittermaier, M., Morcrette, C., Riddick, T., Roberts, M., Sanchez, C., Selwood, P., Stirling, A., Smith, C., Suri, D., Tennant, W., Vidale, P.L., Wilkinson, J., Willett, M., Woolnough, S., Xavier, P., 2017. The Met Office Unified Model Global Atmosphere 6.0/6.1 and JULES Global Land 6.0/6.1 configurations. Geosci. Model Dev. 10, 1487–1520. https://doi.org/10.5194/gmd-10-1487-2017
22. Wilson, D.R., Bushell, Andrew.C., Kerr-Munslow, A.M., Price, J.D., Morcrette, C.J., Bodas-Salcedo, A., 2008. PC2: A prognostic cloud fraction and condensation scheme. II: Climate model simulations. Q. J. R. Meteorol. Soc. 134, 2109–2125. https://doi.org/10.1002/qj.332
23. Do-Yong Kim , Jin-Young Kim , and Jae-Jin Kim, 2012 . A Regression-Based Statistical Correction of Mesoscale Simulations for Near-Surface Wind Speed Using Remotely Sensed Surface Observations. Asia-Pacific J. Atmos. Sci., 48(4), 449-456, 2012 DOI:10.1007/s13143-012-0040-4